

Eur. Phys. J. B **63**, 445–450 (2008)  
DOI: [10.1140/epjb/e2008-00263-1](https://doi.org/10.1140/epjb/e2008-00263-1)

THE EUROPEAN  
PHYSICAL JOURNAL B

# Ab initio cluster calculations of $\text{Co}^{3+}$ spin states in $\text{RBaCo}_2\text{O}_{5.5}$ ( $\text{R} = \text{Ho}, \text{Gd}$ )

L. Siurakshina<sup>1,2,a</sup>, B. Paulus<sup>1,3</sup>, and V. Yushankhai<sup>2,4</sup>

<sup>1</sup> Max-Planck-Institut für Physik Komplexer Systeme, Nöthnitzer Straße 38, 01187 Dresden, Germany

<sup>2</sup> Joint Institute for Nuclear Research, 141980 Dubna, Russia

<sup>3</sup> Physikalische und Theoretische Chemie, Freie Universität Berlin, Takustraße 3, 14195 Berlin, Germany

<sup>4</sup> Max-Planck-Institut für Chemische Physik fester Stoffe, Nöthnitzer Straße 40, 01187 Dresden, Germany

Received 12 February 2008

Published online 10 July 2008 – © EDP Sciences, Società Italiana di Fisica, Springer-Verlag 2008

**Abstract.** Two types of oxygen-deficient perovskites  $\text{RBaCo}_2\text{O}_{5.5}$  ( $\text{R} = \text{Ho}, \text{Gd}$ ) related to the “122” type structure ( $a_p \times 2a_p \times 2a_p$ ) have been studied on the basis of ab initio cluster calculations. We consider the peculiar behavior of the trivalent ions  $\text{Co}^{3+}$  ( $3d^6$ ) in either octahedral or pyramidal oxygen coordinations, which is related to a structural first-order phase transition in both compounds. Relative energy positions of low spin (LS,  $S = 0$ ), intermediate spin (IS,  $S = 1$ ) and high spin (HS,  $S = 2$ ) electron configurations are calculated for the low- and high-temperature lattice structures of  $\text{RBaCo}_2\text{O}_{5.5}$ . A combined analysis of the calculated results and experimental structural data leads to a simple model that captures the most prominent features of the phase transition common to both compounds.

**PACS.** 64.60.Ej – 71.70.-d Level splitting and interactions – 71.15.-m Methods of electronic structure calculations

## 1 Introduction

In the last few years the oxygen-deficient perovskites  $\text{RBaCo}_2\text{O}_{5+x}$ , where  $\text{R}$  is a rare earth atom and  $0 \leq x \leq 1$ , have attracted much attention. This particular family of cobalt oxides shows fascinating physical properties, including giant magneto-resistance [1–4] and large thermoelectric power [5,6], which are promising for their potentially wide applications. At high temperatures, oxygen-deficient cobaltites are interesting also for their high ionic conductivity, thus showing the potential for applications as electrode materials for solid oxide fuel cells.

The physical properties of  $\text{RBaCo}_2\text{O}_{5+x}$  vary strongly in dependence on the oxygen content  $x$ , the sort of rare earth atom  $\text{R}$ , and the applied temperature  $T$ . In contrast to the other  $3d$  transition metal oxides, like cuprates and manganites, in cobaltates the  $\text{Co}$  ions may easily adopt several oxidation states, from  $\text{Co}^{2+}$  to  $\text{Co}^{4+}$ , and within a given valence state, different spin states of the  $\text{Co}^{n+}$  ion may occur including low spin (LS), intermediate spin (IS), and high spin (HS) electronic configurations. The temperature-induced transitions between different  $\text{Co}$ -ion spin states and the related structural lattice changes are provoked by a strong competition between the intra-

atomic exchange interaction ( $\sim J_H$ ) and the crystal field splitting ( $\sim \Delta_{CEF}$ ) of the  $\text{Co}$   $3d$  orbitals in different oxygen coordinations with varying lattice parameters. Therefore, a quantitative characterization of the  $\text{Co}$  spin states with the actual crystal structure of a particular cobalt oxide material is unavoidable in attempting to understand its physical properties. Since the intra-atomic exchange and crystal field effects are of local nature, quantum-chemical cluster calculations are a powerful tool in solving this problem.

Two members of the family  $\text{RBaCo}_2\text{O}_{5+x}$  with  $\text{R} = \text{Ho}, \text{Gd}$  and the oxygen content  $x = 0.5$  are chosen in the present theoretical study involving cluster calculations for small lattice fragments of these compounds. This choice is made because the crystal structures of  $\text{HoBaCo}_2\text{O}_{5.5}$  and  $\text{GdBaCo}_2\text{O}_{5.5}$  have been measured [7,8] in great detail and with high precision.

The compound  $\text{RBaCo}_2\text{O}_{5.5}$  consists of ordered layers  $[\text{CoO}_2]$ - $[\text{BaO}]$ - $[\text{CoO}_2]$ - $[\text{RO}_{0.5}]$  stacked along the  $c$  axis, see Figure 1. The apical oxygen ions and the oxygen vacancies in the  $[\text{RO}_{0.5}]$  layer are ordered in rows parallel to the  $a$  axis and these filled and vacant rows alternate along the  $b$  axis. Thus in this compound ( $Pmmm$  crystal symmetry over a wide temperature range under consideration)  $\text{CoO}_6$  octahedra and  $\text{CoO}_5$  pyramids are ordered and occupy alternating planes along the  $b$  axis. Both the octahedral

<sup>a</sup> e-mail: [siuraksh@jinr.ru](mailto:siuraksh@jinr.ru)

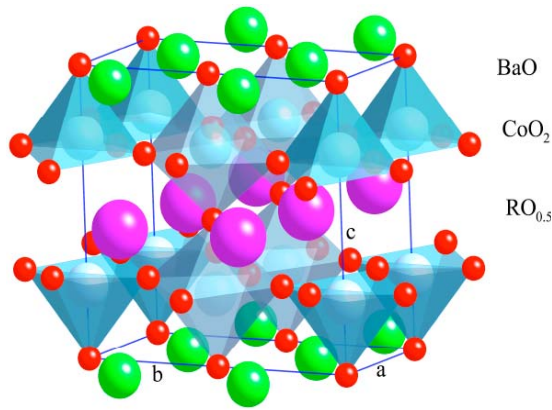


**Fig. 1.** The lattice structure of  $\text{RBaCo}_2\text{O}_{5.5}$  ( $\text{R} = \text{Ho, Gd}$ ); the frame is for elementary cell.

and the pyramidal Co ions are nominally in the 3+ valence state.

Structural phase transitions at  $T_c = 305$  K for  $\text{R} = \text{Ho}$  and  $T_c = 364$  K for  $\text{R} = \text{Gd}$  were reported in references [7,8]. On passing through  $T_c$  in both compounds the lattice symmetry is preserved and the structural transitions consist of a sudden increase of the  $b$  and  $c$  lattice constants,  $\Delta b, \Delta c > 0$ , while  $a$  decreases,  $\Delta a < 0$ . This is accompanied by simultaneous small changes of the Co-O bond lengths and Co-O-Co angles; these internal structural transformations are, however, rather peculiar to  $\text{HoBaCo}_2\text{O}_{5.5}$  or  $\text{GdBaCo}_2\text{O}_{5.5}$ . Though the changes of the lattice constants in both compounds are qualitatively similar, a spread in values of  $\Delta a, \Delta b$ , and  $\Delta c$  results in different volume changes  $\Delta V$  at  $T_c$  on heating. Actually, a unit cell volume contraction,  $\Delta V_0 < 0$ , together with back relaxation in a narrow temperature interval of about 3 K, was detected [8] in  $\text{HoBaCo}_2\text{O}_{5.5}$ . In contrast, the expansion,  $\Delta V_0 > 0$ , for  $\text{GdBaCo}_2\text{O}_{5.5}$  was reported [7]. However, in the latter study the temperature scans near  $T_c$  were done with a much larger temperature step and a possible decrease in volume might not have been detected in  $\text{GdBaCo}_2\text{O}_{5.5}$ . Next, the observed sudden drop at  $T_c$  in the slope of the inverse paramagnetic spin susceptibility  $\chi^{-1}(T)$  and the measured transition enthalpy [8] show that a first-order spin-state transition does occur on Co ions in  $\text{HoBaCo}_2\text{O}_{5.5}$ . A sudden change [7] in  $\chi^{-1}(T)$ , similar to that observed in  $\text{HoBaCo}_2\text{O}_{5.5}$ , indicates that a spin-state transition in  $\text{GdBaCo}_2\text{O}_{5.5}$  is more likely to be of the first-order type as well.

Appearance below  $T_c$  of a superstructure modulation in  $\text{GdBaCo}_2\text{O}_{5.5}$  is reported in reference [9] and interpreted as the unit cell doubling. The measured superstructure reflections with the intensity of  $10^{-4}$  of the basic ones show that the modulation is rather weak and can be neglected in the present study. Below we rely on the structural data, references [7,8], corresponding to the basic  $(a_p \times a_p \times 2a_p)$  structure of  $\text{GdBaCo}_2\text{O}_{5.5}$  and  $\text{HoBaCo}_2\text{O}_{5.5}$  as well.

The temperature dependence of the measured resistivity revealed that in both compounds the structural and spin-state changes at  $T_c$  are accompanied by an insulator-

metal (I-M) transition. The authors of reference [7] attributed the origin of the I-M transition in  $\text{GdBaCo}_2\text{O}_{5.5}$  to a sudden change on heating from Co LS state ( $t_{2g}^6 e_g^0$ ) to HS state ( $t_{2g}^4 e_g^2$ ) in  $\text{CoO}_6$  octahedra, while the Co ions in  $\text{CoO}_5$  pyramids are suggested to remain in the same IS state below and above  $T_c$ . Focusing on  $\text{HoBaCo}_2\text{O}_{5.5}$  the authors of reference [5] applied the concept of spin blockade for the electron transport as a source of the I-M transition and related the mechanism of the spin blockade to a spin-state transition on Co ions. In contrast, the authors of reference [8] insist that the effect of electron delocalization rather than a spin-state transition on Co is responsible for the I-M transition observed in  $\text{HoBaCo}_2\text{O}_{5.5}$ .

The controversy could be resolved on the basis of a microscopic model that includes a set of structural, local spin and itinerant electron degrees of freedom in the system under consideration. Such a model is still lacking. Since a relation between the Co local spin states and structural properties of  $\text{RBaCo}_2\text{O}_{5.5}$  ( $\text{R} = \text{Ho, Gd}$ ) is believed to be at the heart of the problem, a model formulation should be started with a quantitative analysis of this relation.

In our calculations, the main concern is an energy level ordering of different spin states associated with different  $\text{Co}^{3+} 3d^6$ -orbital occupancy below and above the structural phase transition occurring at  $T_c$ . To examine a temperature evolution of the local low-energy spin-state configurations for each compound, with  $\text{R} = \text{Ho}$  and  $\text{Gd}$ , the experimentally determined structural data are taken on both sides of the phase transition. The data contain the lattice constants as well as the internal structural characteristics, including Co-O bond lengths and O-Co-O angles both for  $\text{CoO}_6$  octahedron and  $\text{CoO}_5$  pyramid, which change abruptly at  $T_c$ . A corresponding series of ab initio cluster calculations is performed. The calculated results are analyzed and combined in a model that captures the most prominent features common to the spin-state transitions in both compounds. In fact, we argue below that the desired simplest model is nothing other than the one suggested earlier by Bari and Sivardi re [10]. Within this model, an entropy-driven spin-state transition appears provided the spin-lattice coupling is strong enough. The electron transport properties including the concomitant I-M transition observed in  $\text{HoBaCo}_2\text{O}_{5.5}$  and  $\text{GdBaCo}_2\text{O}_{5.5}$  are fully beyond the scope of the model. This complicated problem is not touched in the present study.

## 2 Ab initio calculations

### 2.1 Selection of clusters

To apply highly accurate quantum chemical methods it is necessary to mimic the extended solid with properly embedded finite clusters. Due to our interest in the local Co spin states, we select Co-centered clusters, in particular the two clusters (see Fig. 2) with the oxygen ions surrounding octahedrally or pyramidally the central  $\text{Co}^{3+}$ . In both cases, the bare fragments  $[\text{CoO}_6]^{9-}$  and  $[\text{CoO}_5]^{7-}$  are supplemented with four  $\text{Ba}^{2+}$  and four  $\text{R}^{3+} = \text{Ho}^{3+}/\text{Gd}^{3+}$

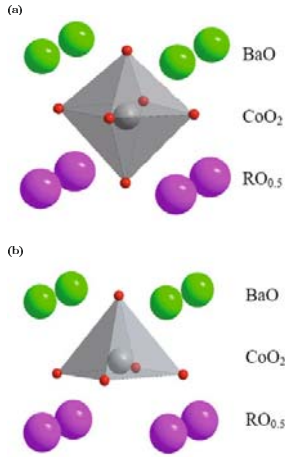


**Fig. 2.** Choice of the clusters  $[\text{R}_4\text{Ba}_4\text{CoO}_6]^{11+}$  and  $[\text{R}_4\text{Ba}_4\text{CoO}_5]^{13+}$  for  $\text{Co}^{3+}$  in the octahedral (a) and the pyramidal (b) oxygen coordinations.

cations. Additional to these fully described atoms the clusters are embedded in a point-charge array (1240/1239 point charges for the two clusters respectively) which simulates the electrostatic potential of the crystal. These point charges have the formal ionic charge in the interior of the array and are reduced by a factor of 2 at faces, a factor of 4 at edges and a factor of 8 at corners of the array (Evjens method). Test calculations show, that the size of the point charge array is sufficiently large.

To examine the Co spin states at the experimentally observed lattice structure both below and above the transition temperature  $T_c$ , we selected two sets of the lattice parameters for our calculations, namely the experimentally measured values [7,8] at  $T \simeq 250 \text{ K} < T_c$  and at  $T \simeq 350 \text{ K} > T_c$  for  $\text{HoBaCo}_2\text{O}_{5.5}$ , and  $T \simeq 300 \text{ K} < T_c$  and at  $T \simeq 400 \text{ K} > T_c$  for  $\text{GdBaCo}_2\text{O}_{5.5}$ . Taken not too close to  $T_c$ , the selected structural data provide a better contrast between the properties calculated in the low-temperature (LT) and the high-temperature (HT) phases. The point charge array is also modified according to the chosen lattice structure.

## 2.2 Quantum chemical methods

For each cluster chosen, the energies of the lowest electron configurations in the different spin states  $S = 0, 1, 2$  were calculated at different levels of accuracy: due to the fact that one has to distribute six electrons of  $\text{Co}^{3+}$  in five  $d$  orbitals only a multi-configuration self-consistent field ansatz (MCSCF) [11,12] is sensible, where at least all five  $d$  orbitals are in the active space. The remaining occupied orbitals of the clusters can be treated as closed shell orbitals with fixed occupancy of 2. However test calculations show, that it is important to reoptimize the occupied  $4s^2$  and the  $3s^2p^6$  during the MCSCF procedure, because these orbitals are strongly affected by the changes in the occupation of the different spatial  $3d$  orbitals. The other occupied orbitals can be kept unchanged

from the orbitals obtained with a single-reference Hartree-Fock method. On top of this MCSCF treatment which can describe the static correlations, the dynamical correlations (virtual excitations into unoccupied orbitals of the whole cluster) are calculated with the multi-reference configuration method (MRCI) allowing all single and double excitations [13–15] from the MCSCF solution. In this procedure the orbital coefficients are kept fixed at the MCSCF level. The calculations are performed with the quantum chemical programme package MOLPRO [16].

## 2.3 Pseudopotentials and basis sets

To reduce the number of electrons in the calculation the core electrons are described with pseudopotentials. For the Co atom, the inner ten electrons (Ne core) are simulated with a scalar relativistic energy-consistent effective core potential [17] yielding 14 electrons to be explicitly calculated for  $\text{Co}^{3+}$ . Concerning the Ba atom, an effective core potential with a  $\text{Kr} + 4d^{10}$  core was used [18], leaving for each  $\text{Ba}^{2+}$  the 8 electrons in the closed semi-core  $5s^2p^6$  shell for the calculation. The rare earth atoms Ho and Gd are modeled with effective core potentials, where the partial occupied  $f$  shell is in the core [19]. This is a good approximation for the problems we are considering, because we are not interested in the spin state of the rare earth atoms and the  $f$  shells are well localized at the rare earth atoms and have therefore no influence on the surroundings of the Co-atom. Magnetic interactions between the Co spin moment and the rare earth spin moment are expected to be much smaller than the on-site spin interaction of Co. The spatially most extended orbitals of the rare earth atoms are the  $5s^2p^6$  orbitals, whose electrons are treated explicitly to allow for non-spherical arrangement due to hybridization according to the lattice structure.

To model numerically the Hilbert space of the system we select as basis atom-centered basis functions, which are described as linear combinations of contracted Gaussian-type orbitals. For the remaining electrons at the Co-site we use a basis  $[6s5p3d2f]$  contracted from a  $(8s7p6d2f)$  primitive basis set [17]. For the O atoms we apply a correlation consistent basis set of valence-double  $\zeta$  quality with one  $d$  polarization function [20]. At the outer atoms in the cluster, a basis  $[2s2p]$  (Refs. [18,19]) is supplied, optimized for the pseudopotentials described above. We have tested this choice of the basis set carefully. Whereas the total energies change significantly with improving basis set the splitting between the different spin states stays quite constant. An error estimation of the limited basis set on the level splitting of 0.2 eV is reasonable.

## 2.4 Results of the ab initio cluster calculations

The low-energy electron configurations with  $S = 0, 1$  and 2 are selected and their energies are obtained from the MRCI calculations for the two clusters shown in Figure 2. Different spin states are associated with different  $\text{Co}^{3+}$

**Table 1.** The calculated relative energy positions (in eV) of low-energy cluster electron configurations with different spin  $S$  for the low-temperature (LT) and the high-temperature (HT) structural phases of  $\text{HoBaCo}_2\text{O}_{5.5}$  and  $\text{GdBaCo}_2\text{O}_{5.5}$ .

$\text{HoBaCo}_2\text{O}_{5.5}$		$\text{CoO}_6$		$\text{CoO}_5$		$\text{GdBaCo}_2\text{O}_{5.5}$		$\text{CoO}_6$		$\text{CoO}_5$	
	$S$	LT	HT	LT	HT		$S$	LT	HT	LT	HT
	0	0	1.7	0.8	0.3		0	0	1.5	1.1	0.31
	1	3.1	1.0	$\approx 0$	0		1	2.2	1.0	0	0
	2	2.7	0	$\approx 0$	0.5		2	1.2	0	0.5	0.48

3d-orbital occupancy in the LT phase, at  $T < T_c$ , or in the HT one, at  $T > T_c$ .

In Table 1, the calculated relative energy positions of different cluster spin states are shown for both compounds in the LT and HT phases. Here, the cluster  $[\text{R}_4\text{Ba}_4\text{CoO}_6]/[\text{R}_4\text{Ba}_4\text{CoO}_5]$  is denoted as  $\text{CoO}_6/\text{CoO}_5$  respectively and the energies of the calculated ground state spin multiplets are set to zero. It is worth comparing now the patterns of the spin-state level ordering calculated for  $\text{HoBaCo}_2\text{O}_{5.5}$  and  $\text{GdBaCo}_2\text{O}_{5.5}$ . Considering either  $\text{CoO}_6$  or  $\text{CoO}_5$ , one may see a close similarity between the corresponding patterns in both compounds; one prominent distinction is also present. Let us discuss this issue in more detail.

In  $\text{GdBaCo}_2\text{O}_{5.5}$  the ground state  $S = 0$  configuration of  $\text{CoO}_6$  in the LT phase changes into one with  $S = 2$  in the HT phase, while the lowest  $S = 1$  state of  $\text{CoO}_5$  remains in both phases. This behavior is compatible with that derived from experimental observation on  $\text{GdBaCo}_2\text{O}_{5.5}$  as reported in reference [7]. In the HT phase of  $\text{HoBaCo}_2\text{O}_{5.5}$ , the level ordering is similar qualitatively to that of  $\text{GdBaCo}_2\text{O}_{5.5}$ . That is also true for the LT level structure in  $\text{CoO}_6$ , but not in  $\text{CoO}_5$ . Instead of well separated energy levels, the calculated energy difference between the two lowest spin states,  $S = 2$  and  $S = 1$ , of the pyramidal Co ion in  $\text{HoBaCo}_2\text{O}_{5.5}$  is found to be  $\sim 0.03$  eV, with  $S = 2$  configuration being more stable. This small energy difference is, however, within the error of the present calculations. Therefore, what we may conclude at the most is that the two lowest configurations are quasi-degenerate.

In both compounds, the most prominent effect of changing the lattice parameter on the cluster spin state is found for  $\text{CoO}_6$  clusters. In this respect, the energy difference  $\Delta$  between the LS ground state and the first excited HS state of a  $\text{CoO}_6$  cluster in the LT phase is of special interest. We note that the calculated values, namely,  $\Delta = 2.7$  eV for  $\text{HoBaCo}_2\text{O}_{5.5}$  and  $\Delta = 1.2$  eV for  $\text{GdBaCo}_2\text{O}_{5.5}$ , are surprisingly large. Nevertheless, as the structural lattice parameters are relaxed to those of the HT phase, the calculations lead immediately to a reversal of the HS-LS energy separation. Since the corresponding structural parameter changes are not large, but rather moderate, one may conclude that the relative energies of the different spin states of the  $\text{CoO}_6$  cluster are very sensitive to variations of the lattice structure.

The total energy of an octahedral/pyramidal cluster embedded in a lattice of point charges can be written as  $E_{\text{tot}} = E^{\text{oct/pyr}} + W^{\text{oct/pyr}}$ . Here,  $E^{\text{oct/pyr}}$  is the cluster electronic energy (one-electron and two-electron terms), including the Coulomb interaction of the cluster electrons

with the embedding lattice;  $W^{\text{oct/pyr}}$  is the Coulomb energy of the cluster ionic core centers interacting among themselves and with the point-charge lattice. The electronic part of cluster ground state energies,  $E_{\text{HT}}^{\text{oct/pyr}}$  and  $E_{\text{LT}}^{\text{oct/pyr}}$ , calculated for  $\text{CoO}_6/\text{CoO}_5$  with the HT and LT structural parameters, respectively, are of special importance. To get more insight into the spin-state transition in question, we calculated the energy changes,  $\Delta E^{\text{oct}} = E_{\text{HT}}^{\text{oct}} - E_{\text{LT}}^{\text{oct}}$  and  $\Delta E^{\text{pyr}} = E_{\text{HT}}^{\text{pyr}} - E_{\text{LT}}^{\text{pyr}}$ , and found a similar behavior, namely, the electronic energy lowering,  $\Delta E^{\text{oct}} < 0$ , for the octahedral cluster and the increase,  $\Delta E^{\text{pyr}} > 0$ , for the pyramidal one, in both compounds. From this observation, one may conclude that the electron density redistribution in  $\text{CoO}_6$  connected to structural and spin state transitions promotes these transitions, while that occurring in  $\text{CoO}_5$  tends to inhibit them. This result gives additional support to the view that the octahedrally coordinated Co ions play a dominant role in the observed transitions. In the next section, these findings are involved in an appropriate microscopic model which enable us to give a qualitative account of these transitions.

### 3 Discussion and interpretation of the data with a model Hamiltonian

For both compounds under consideration, the calculated results, Table 1, reveal a similar rearrangement of the Co spin-state level ordering as the LT lattice structure is switched over to the HT one. It is tempting now to search for a common model which relates the relevant lattice and spin degrees of freedom for both compounds on an equal ground. Such a common model does not attempt to account for many peculiarities particular to either  $\text{HoBaCo}_2\text{O}_{5.5}$  or  $\text{GdBaCo}_2\text{O}_{5.5}$ . For instance, a variation of the energy level position of Co spin states allied to a weak temperature evolution of the lattice structures below and above  $T_c$  is not traced out. Also, electronic transport properties including a subsidiary I-M transition triggered by a sudden spin state change on Co ions are obviously beyond the scope of the model. Our main goal is to highlight the most general aspects of the spin-state and structural phase transitions of interest. In this search we found that the simplest desired model can be taken in the form suggested earlier [10] by Bari and Sivardi re (BS). This argument goes as follows:

First, recalling results of Section 2, a dominant role of the octahedral Co ions has to be emphasized once more. Actually, the simulation of temperature-induced lattice structure changes in our calculations results in the LS-HS



transition and a concomitant lowering of the electronic energy in the  $\text{CoO}_6$  cluster. In contrast, no prominent spin changes and an increase of the electronic energy under the actual structural lattice changes are seen from the  $\text{CoO}_5$  cluster calculations. Thus, having no active spin degrees of freedom, the pyramidal Co ions can be regarded as contributing mainly to the elastic energy of a lattice deformation related to the LS-HS transition in the system. The active LS and HS states of the  $i$ -th octahedral Co ion are associated below with the occupation number  $n_i = 0$  or  $n_i = 1$ , respectively. The third, i.e. IS state is irrelevant, and thus we may restrict our analysis to a two-state ionic problem according to the BS model.

Homogeneous lattice deformation related to the LS-HS transition in both compounds can be described by a diagonal deformation matrix  $\mathbf{u}$ . As a measure  $Q$  of the deformation, any of the diagonal elements, say,  $Q = u_{11}$ , can be taken. Then, in general, one may write down  $u_{22} = -\sigma_2 Q$  and  $u_{33} = -\sigma_3 Q$ , where coefficients  $\sigma_{2,3}$  are simply connected to the measured changes of lattice constants. Connected to the lattice deformation a relative unit-cell volume expansion (contraction) is  $\Delta V_0/V_0 = (1 - \sigma_2 - \sigma_3) Q$ . The elastic energy per unit cell is quadratic in  $u_{ii}$ :  $\mathcal{E} = (1/2) \sum_{ij} k_{ij} u_{ii} u_{jj}$ , where  $k_{ij} (= k_{ji})$  are the elastic moduli of the orthorhombic lattices under consideration. With the above assumptions, the elastic energy can be written as  $\mathcal{E} = KQ^2/2$ , where  $K > 0$  is a material dependent effective force constant.

In a frozen lattice,  $Q = 0$ , the excited HS state of each octahedral Co ion is separated from the ground LS state by an energy gap  $\Delta > 0$ ; the existing crystal field effects dominate the intra-atomic exchange to give the electronic ground state configuration with  $n_i = 0$  on each active site over the lattice. As temperature increases, thermal population of the HS state accompanied with a lattice deformation,  $Q \neq 0$ , reduces the HS-LS energy separation to a value  $(\Delta - \lambda Q)$ ; the reduction is assumed to be linear in  $Q$  with  $\lambda$  denoting an effective spin-lattice coupling constant. For a relaxed lattice in the HT phase, one has  $(\Delta - \lambda Q) < 0$ , which implies the above-mentioned electronic energy lowering in  $\text{CoO}_6$  clusters. This energy gain due to the LS-HS transition on the octahedral Co ions competes with the elastic energy of the concomitant lattice deformation. In this simplest possible scenario for the LS-HS transition, a detailed knowledge of internal structural characteristics, including the Co-O bond lengths and O-Co-O angles in  $\text{CoO}_6$  octahedron, is not required. Instead, a properly chosen variable  $Q$  is assumed to be the only essential parameter of a lattice deformation connected to the LS-HS transition.

The Hamiltonian of the system can now be written as [10]

$$H = N \frac{K}{4} Q^2 + \sum_i^N (\Delta - \lambda Q) n_i, \quad (1)$$

where  $N$  is the number of octahedral Co ions in the system. As noted in reference [10], the Hamiltonian (1) can be also regarded as that emerging from a mean-field treat-

ment of a lattice two-state ionic model with the infinite-range pair-spin interaction mediated by a lattice distortion that is treated classically.

With the Hamiltonian (1) the free energy per active Co ion is given by

$$F = \frac{K}{4} Q^2 - \beta^{-1} \ln \left[ 1 + \nu e^{-\beta(\Delta - \lambda Q)} \right], \quad (2)$$

where  $\beta = 1/k_B T$  ( $k_B$  is the Boltzmann constant) and  $\nu > 1$  is the multiplicity of the ionic HS state. In the present case, because the cubic symmetry of the octahedral surrounding of Co ions is strongly perturbed, we adopt  $\nu = 5$  for  $S = 2$ . In fact, the overall picture of the LS-HS transition emerging from the model is qualitatively similar for any integer  $\nu > 1$ . This can be summarized briefly as follows. For the dimensionless parameter  $\xi = \lambda^2 / K \Delta$  ranging in  $0 < \xi_c < \xi < 1$ , a first-order LS-HS phase transition with a step-like increase of the HS state occupancy together with a sudden change of  $Q$  (and of the sample volume) is predicted to occur on heating. Here, the lower threshold value  $\xi_c$  varies with  $\nu$  and, for instance,  $\xi_c \approx 0.55$  if  $\nu = 5$ . The predicted transition temperature  $T_c = \Delta(1 - \xi) / (k_B \ln \nu)$  decreases with increasing  $\xi$  and tends to zero as  $\xi \rightarrow 1$ . For  $\xi > 1$ , the system would be unstable with respect to the LS-HS transition already at  $T = 0$ . Taking into account the estimate,  $\Delta \sim 2$  eV and  $T_c \sim 300$  K, one obtains  $\xi \approx 0.98$ , which implies a strong spin-lattice coupling and a proximity of the system to the instability.

Finally, we note that slightly extended versions of the model were recently applied to describe spin-state transitions in the perovskite  $\text{LaCoO}_3$  [21] and octahedral Fe-complexes [22] having  $d^6$  electron configurations.

## 4 Conclusion

In the present work, ab initio quantum chemical cluster methods were employed to study temperature-induced spin-state transitions observed in cobalt oxides  $\text{RBaCo}_2\text{O}_{5.5}$  ( $R = \text{Ho}, \text{Gd}$ ). For each compound, two characteristic sets of structural lattice parameters, experimentally determined in the low-temperature and the high-temperature phases, were selected and the corresponding energy level ordering of  $\text{Co}^{3+}$  spin states, below and above the transition temperature  $T_c$ , were evaluated by means of cluster calculations; Co ions with the octahedral and the pyramidal oxygen coordinations were examined separately. The calculations supported the expected result that the lowest spin state of the  $\text{CoO}_6$  cluster is extremely sensitive to the actual changes of the lattice structure, in contrast to the behavior obtained for the  $\text{CoO}_5$  cluster spin states. The dominant role of the octahedral Co ions in the spin-state transitions in both compounds was also supported by a supplementary cluster analysis of the evaluated electronic energy changes accompanying the structural changes in  $\text{RBaCo}_2\text{O}_{5.5}$  ( $R = \text{Ho}, \text{Gd}$ ). With these findings, we argued next that the most general aspects of the first-order phase transition in these rather complex

compounds could be understood based on a simple model treating the transition as a spin-entropy driven one.

In view of very complicated behaviour the system shows at the phase transition, the presented model is obviously not sufficient. First, the performed quantitative analysis of an isolated cluster enabled us to obtain only a bare value of the LS-HS energy gap  $\Delta$  in the LT phase. The calculated  $\Delta$  was found to be surprisingly large, especially in  $\text{HoBaCo}_2\text{O}_{5.5}$ , Table 1. In fact, below  $T_c$  thermal excitation of the HS state in the lattice system means an injection of an electron to the bottom of a broad  $e_g$  band with a holes left at the top of a narrower  $t_{2g}$  band. This banding effect reduces the actual LS-HS gap to a value which is smaller than the calculated one. Second, the internal structural characteristics, including the Co-O bond lengths and Co-O-Co angles, together with their temperature changes at  $T_c$ , are not considered explicitly in the suggested simple model. In fact, several of the omitted lattice degrees of freedom and the observed insulator-metal transition are expected to be closely related to each other. As noted, for instance, in reference [8], at the transition temperature  $T_c$  a step-like increase of the electron transfer integral  $t$  is expected to be a result of a sudden increase of Co-O-Co angles observed along particular Co-O bond directions. This additional temperature-induced bandwidth broadening of the excited HS energy level implies a further reduction of the LS-HS energy gap to a smaller value  $\Delta_{\text{eff}} < \Delta$ , compared with the bare  $\Delta$  calculated for an isolated cluster with a rigid LT lattice structure. Related to the bandwidth broadening, a kinetic energy lowering of the conducting electrons in  $e_g$  band may be regarded as an extra source that promotes the overall instability of the system when approaching to the transition temperature  $T_c$ . We suggest, however, that the driving force for the phase transition is mainly due to the spin-state instability of the octahedral Co ions, while the electron kinetic energy lowering is a subsidiary effect. It is worth noting that the insertion of the actual gap value  $\Delta_{\text{eff}}$  into the expression for the spin-state transition temperature  $T_c$  derived in the proceeding section would soften a strong constraint on a strength of the spin-lattice coupling  $\xi$ . Next, rather unusual for the LS-HS transition the unit-cell volume contraction at  $T_c$  and its subsequent back relaxation in narrow temperature interval above  $T_c$  found in  $\text{HoBaCo}_2\text{O}_{5.5}$  is probably due to a special anisotropic mechanism of electron delocalization. We note that for temperatures well above  $T_c$ , a net effect of the LS-HS transition in both compounds is a unit-cell expansion compatible with a larger ionic radius of  $\text{Co}^{3+}$  in the HS state.

To combine the above effects in a unified picture, a properly extended model should include the itinerant electron degrees of freedom and a more detailed treatment of the lattice dynamics, together with the main features of the suggested simple model. Within the extended model

one has to describe how the abrupt changes in the properties of  $\text{RBaCo}_2\text{O}_{5.5}$  are related and triggered by the underlying spin-state instability of the octahedral Co ions.

We would like to thank Dr. V. Pomjakushin (ETHZ and PSI, Villigen) for information about the crystal structure data for  $\text{HoBaCo}_2\text{O}_{5.5}$ .

## References

1. C. Martin, A. Maignan, D. Pelloquin, N. Nguyen, B. Raveau, *Appl. Phys. Lett.* **71**, 1421 (1997)
2. M. Respaud, C. Frontera, J.L. Garcia-Muñoz, M.Á.G. Aranda, B. Raquet, J.M. Broto, H. Rakoto, M. Goiran, A. Llobet, J. Rodríguez-Carvajal, *Phys. Rev. B* **64**, 214401 (2001)
3. A.A. Taskin, A.N. Lavrov, Y. Ando, *Phys. Rev. Lett.* **90**, 227201 (2003)
4. D.D. Khalyavin, S.N. Barilo, S.V. Shiryayev, G.L. Bychkov, I.O. Troyanchuk, A. Furrer, P. Allenspach, H. Szymczak, R. Szymczak, *Phys. Rev. B* **67**, 214421 (2003)
5. A. Maignan, V. Caignaert, B. Raveau, D. Khomskii, G. Sawatzky, *Phys. Rev. Lett.* **93**, 026401 (2004)
6. A.A. Taskin, Y. Ando, *Phys. Rev. Lett.* **95**, 176603 (2005)
7. C. Frontera, J.L. Garcia-Muñoz, A. Llobet, M.A.G. Aranda, *Phys. Rev. B* **65**, 180405 (2002)
8. E. Pomjakushina, K. Coder, V. Pomjakushin, *Phys. Rev. B* **73**, 113105 (2006)
9. Yu. Chernenkov, V. Plakhty, V. Fedorov, S. Barilo, S. Shiryayev, G. Bychkov, *Phys. Rev. B* **71**, 184105 (2005)
10. R. Bari, J. Sivadère, *Phys. Rev. B* **5**, 4466 (1972)
11. H.-J. Werner, P.J. Knowles, *J. Chem. Phys.* **82**, 5053 (1985)
12. P.J. Knowles, H.-J. Werner, *Chem. Phys. Lett.* **115**, 259 (1985)
13. S.R. Langhoff, E.R. Davidson, *Intern. J. Quantum Chem.* **8**, 61 (1974)
14. H.-J. Werner, P.J. Knowles, *J. Chem. Phys.* **89**, 5803 (1988)
15. P.J. Knowles, H.-J. Werner, *Chem. Phys. Lett.* **145**, 514 (1988)
16. MOLPRO, version 2006.1, a package of ab initio programs, H.-J. Werner, P.J. Knowles, R. Lindh, F.R. Manby, M. Schütz, and others, see <http://www.molpro.net>
17. M. Dolg, U. Wedig, H. Stoll, H. Preuss, *J. Chem. Phys.* **86**, 866 (1987)
18. M. Kaupp, P.V.R. Schleyer, H. Stoll, H. Preuss, *J. Chem. Phys.* **94**, 1360 (1991)
19. M. Dolg, H. Stoll, A. Savin, H. Preuss, *Theor. Chim. Acta* **75**, 173 (1989)
20. Dunning, T.H. Jr, *J. Chem. Phys.* **90**, 1007 (1989)
21. R.P.G. Radaelli, S.-W. Cheong, *Phys. Rev. B* **66**, 094408 (2002)
22. S.W. Biernacki, B. Clerjaud, *Phys. Rev. B* **72**, 024406 (2005)